Myoglobin translational diffusion in rat myocardium and its implication on intracellular oxygen transport

Ping-Chang Lin, Ulrike Kreutzer and Thomas Jue

Department of Biochemistry and Molecular Medicine, University of California Davis, Davis, CA 95616-8635, USA

Current theory of respiratory control invokes a role of myoglobin (Mb)-facilitated O_2 diffusion in regulating the intracellular O_2 flux, provided Mb diffusion can compete effectively with free O_2 diffusion. Pulsed-field gradient NMR methods have now followed gradient-dependent changes in the distinct ^{1}H NMR γ CH_3 Val E11 signal of MbO_2 in perfused rat myocardium to obtain the endogenous Mb translational diffusion coefficient (D_{Mb}) of 4.24×10^{-7} cm^2 s^{-1} at 22°C. The D_{Mb} matches precisely the value predicted by *in vivo* NMR rotational diffusion measurements of Mb and shows no orientation preference. Given values in the literature for the Krogh's free O_2 diffusion coefficient (K_0), myocardial Mb concentration and a partial pressure of O_2 that half saturates Mb (P_{50}), the analysis yields an equipoise diffusion P_{O_2} of 1.77 mmHg, where Mb and free O_2 contribute equally to the O_2 flux. In the myocardium, Mb-facilitated O_2 diffusion contributes increasingly more than free O_2 diffusion when the P_{O_2} falls below 1.77 mmHg. In skeletal muscle, the P_{O_2} must fall below 5.72 mmHg. Altering the Mb P_{50} induces modest change. Mb-facilitated diffusion has a higher poise in skeletal muscle than in myocardium. Because the basal P_{O_2} hovers around 10 mmHg, Mb does not have a predominant role in facilitating O_2 transport in myocardium but contributes significantly only when cellular oxygen falls below the equipoise diffusion P_{O_2}.

(Received 26 June 2006; accepted after revision 5 October 2006; first published online 12 October 2006)
Corresponding author T. Jue: Department of Biochemistry and Molecular Medicine, University of California Davis, Davis, CA 95616-8635, USA. Email: tjue@ucdavis.edu

A cornerstone of respiratory regulation stands on the capacity of myoglobin (Mb) to store O_2 or to facilitate O_2 transport. In marine mammals, the high concentration of Mb could certainly supply O_2 during a dive or apnoea (Dolar *et al.* 1999; Guyton *et al.* 1995; Kooyman, 1998; Ponganis *et al.* 2002). In adaptation to high altitude, enhanced Mb expression increases the O_2 depot (Gimenez *et al.* 1977; Terrados *et al.* 1990). These observations agree with the correlation between Mb concentration (O_2 supply) and oxidative capacity in different species (Wittenberg & Wittenberg, 2003). Yet, in spontaneously beating rat heart, Mb can prolong normal heart function for only a few seconds (Chung & Jue, 1996). Without any Mb, neither myocardial nor skeletal muscle function suffers any apparent physiological impairment (Garry *et al.* 1998; Godecke *et al.* 1999).

The physiology canon also states that Mb can facilitate O_2 diffusion. In contrast to the low solubility of O_2, the high O_2 carrying capacity of Mb can confer an advantage in transporting O_2 from the sarcolemma to the mitochondria (Wittenberg, 1970; Wittenberg & Wittenberg, 1989). *In vitro* studies have confirmed that O_2 diffuses faster in solution containing Mb than in Mb-free solution. Mb exhibits sufficient mobility and O_2 carrying capacity to compete effectively with free O_2 (Johnson *et al.* 1996). *In vivo*, however, the contribution of Mb-facilitated O_2 diffusion remains unclear. Without a definitive translational diffusion coefficient for Mb (D_{Mb}) *in vivo*, the theory of Mb-facilitated diffusion languishes for experimental confirmation.

Over the years, researchers have attempted to estimate endogenous Mb diffusion in the cell by measuring Mb diffusion in concentrated solution, in tissue homogenate and in myoglobin-free frog muscle (Moll, 1968; Riveros-Moreno & Wittenberg, 1972; Baylor & Pape, 1988). The results have varied widely. Fluorescence recovery after photobleaching (FRAP) techniques have recently tracked the photoxidation of Mb in superfused rat diaphragm or the diffusion of microinjected modified Mb in isolated muscle fibre. These experiments have determined a low D_{Mb} that cannot support any significant role for Mb in facilitating O_2 diffusion (Jurgens *et al.* 1993; Papadopoulos *et al.* 2001).

However, the FRAP experiments do not actually measure endogenous Mb diffusion and utilize model systems that do not adequately mimic respiring tissue

 DOI: 10.1113/jphysiol.2006.116061

(Groebe, 1995). Moreover, they disagree with the *in vivo* NMR observation of Mb rotational diffusion, which predicts a much faster D_{Mb} (Livingston *et al.* 1983; Wang *et al.* 1997).

Because the ^{1}H NMR can detect the distinct γCH_3 Val E11 signal of MbO_2 in myocardium at −2.8 ppm, an opportunity exists to apply pulsed-field gradient technique to map endogenous Mb translational diffusion in perfused myocardium (Stejskal & Tanner, 1965; Kreutzer *et al.* 1992). Indeed, MbO_2 diffuses with an average coefficient about 4 times faster than the FRAP-determined diffusion coefficient and shows no orientation preference. The D_{Mb} also matches precisely the value predicted by the NMR rotational diffusion analysis (Wang *et al.* 1997).

Given the Mb concentration in tissue, the partial pressure of O_2 that half saturates Mb (P_{50}) and the D_{Mb}, the analysis establishes an equipoise diffusion P_{O_2} in the cell, where Mb and free O_2 contribute equally to O_2 transport. In the basal state rodent myocardium or skeletal muscle, Mb cannot play a significant role in facilitating O_2 diffusion. In contrast, marine mammal muscle with a high Mb concentration can utilize Mb-facilitated O_2 diffusion under all physiological conditions. The conclusion agrees with Mb studies in which rat myocardium inhibited with a significant fraction of CO-bound Mb exhibits no sign of respiration or metabolism impairment (Glabe *et al.* 1998; Chung *et al.* 2006). The NMR-determined translational diffusion coefficient of endogenous Mb in respiring myocardium has established a key parameter that does not lend support to the hypothesis that Mb has an overall general role in facilitating O_2 transport in respiring tissue. Instead, the D_{Mb} defines the physiological conditions in which Mb can contribute significantly to the intracellular O_2 flux.

Methods

Protein preparation

Mb solution was prepared from lyophilized horse heart protein (Sigma Chemical Inc.). The preparation of MbCO solution followed the procedure previously described (Kreutzer *et al.* 1993). The same process was also applied to prepare the haemoglobin (Hb) solution, in which Hb was extracted from human erythrocytes (Wang *et al.* 1997).

Animal preparation and heart perfusion

Animal care and experimental procedures followed the guidelines of the NIH Office for Laboratory Animal Welfare and were approved by the University of California Davis Institutional Animal Use and Care Committee. The procedure for rat heart perfusion was performed as previously described (Chung & Jue, 1999; Kreutzer & Jue, 2004). Male Sprague-Dawley rats (350–400 g) were anaesthetized by an intraperitoneal injection of sodium pentobarbital (65 mg kg^{-1}) and heparinized (1000 U kg^{-1}). The heart was quickly isolated and perfused in Langendorff perfusion apparatus, with Krebs-Henseleit buffer maintained at room temperature (21–23°C). A peristaltic pump (Rainin Rabbit) maintained a constant, non-recirculating perfusion flow of 12–13 ml min^{-1}.

K^+-induced arrest

After a 20 min control period, the perfusate was switched to Krebs-Henseleit buffer containing 92.7 mM NaCl and 30 mM KCl, which stopped the heart beat. The perfusate flow rate was reduced to 50% of control 10 min after the heart stopped beating. High K^+ perfusion continued for approximately 7 h. The perfusate was then switched back to 118 mM NaCl, 4.7 mM KCl, and the flow returned to its control level. Perfusion then continued for 20–30 min.

NMR

An Avance 400-MHz Bruker spectrometer measured the ^{1}H/^{31}P signals with a 20 mm micro-imaging gradient probe. The ^{1}H 90 deg pulse was 65 μs. A modified Stejskal-Tanner pulsed-field gradient spin echo or pulsed-field gradient stimulated echo (PG-STE) sequence followed the Val E11 resonance of MbCO and MbO_2 at −2.4 ppm and −2.8 ppm, respectively (Stejskal & Tanner, 1965; Price, 1997). The gradient field strength ranged from 0 to 95 G (gauss cm^{-1}). A typical spectrum required 1024 scans and used the following signal acquisition parameters: 8192 Hz spectral width, 4096 data points and 255 ms acquisition time. The H_2O line served as the spectral reference, 4.75 ppm at 25°C relative to sodium-3-(trimethylsilyl)propionate-2,2,3,3-d4 at 0 ppm

Diffusion measurements in perfused heart experiments utilized a modified PG-STE sequence that included chemical-shift selective (CHESS) pulses (Haase *et al.* 1985). For the diffusion measurements, the acquisition parameters included the following: acquisition time of 38.5 ms, spectral width of 10 KHz and 768 data points. A typical spectrum required 16 000 scans or about 24 min of signal accumulation.

For the ^{31}P spectra, the signal acquisition utilized a 55 deg pulse angle, 6494 Hz spectral width, 4096 point data size and a 0.65 s repetition time. The ^{31}P 90 deg pulse was 72 μs calibrated against a 0.1 M phosphate solution. Peak area analysis, calibrated against fully relaxed spectra, determined the phosphocreatine (PCr) and ATP levels. All ^{31}P signals were referenced to PCr peak as 0 ppm A typical spectrum required 256 scans.

Diffusion equation

The NMR determination of the translational diffusion relates signal intensity change with strength of the applied rectangular gradient pulses (Stejskal & Tanner, 1965; Price, 1997):

$$\ln\left(\frac{S(G)}{S(0)}\right) = -\gamma^2\delta^2(\Delta-\delta/3)G^{\mathrm{T}}DG = -\sum_{i=1}^{3}\sum_{j=1}^{3}\gamma^2\delta^2(\Delta-\delta/3)G_iD_{ij}G_j = -\sum_{i=1}^{3}\sum_{j=1}^{3}b_{ij}D_{ij} \quad (1)$$

where S(G) is the signal intensity in an applied field gradient, $S(0)$ is the signal intensity with no applied field gradient, γ is the magnetogyric ratio, δ is the duration of the gradient pulse, Δ is the gradient pulse separation, G and G^{T} are the 1×3 and 3×1 gradient field tensor and its transpose, D is the 3×3 rank-two diffusion tensor and G_{i}, G_{j} and D_{ij} are the respective matrix elements. The equation reduces to a linear combination of the product of tensor elements D_{ij} and b_{ij}, where

$$b_{\mathrm{ij}} = \gamma^2G_iG_j\delta^2(\Delta-\delta/3) \quad (2)$$

To determine molecular diffusion requires measuring the signal intensity as a function of gradient pulses G applied along different directions, reflecting the elements of the b matrix. In the case of isotropic diffusion, the observations corresponding to diagonal elements will not differ, and the equation reduces to a simple expression:

$$\mathrm{In}\left(\frac{S(G)}{S(0)}\right) = -bD = -\gamma^2G^2\delta^2(\Delta-\delta/3)D \quad (3)$$

O_2 transport by Mb and free diffusion

The relative O_2 flux by Mb-facilitated diffusion and free O_2 derives from following equations:

$$F_{\mathrm{O_2}} = F_{\mathrm{O_2}}^{\mathrm{Mb}} + F_{\mathrm{O_2}}^{\mathrm{O_2}} \quad (4)$$

$$F_{\mathrm{O_2}}^{\mathrm{Mb}} = \frac{D_{\mathrm{Mb}}C_{\mathrm{Mb}}P_{50}}{(P_{\mathrm{O_2}}+P_{50})(P_{\mathrm{r}}+P_{50})}\cdot\frac{\Delta P}{\Delta x} \approx \frac{D_{\mathrm{Mb}}C_{\mathrm{Mb}}}{P_{\mathrm{O_2}}+P_{50}}\cdot\frac{\Delta P}{\Delta x} \quad (5)$$

$$F_{\mathrm{O_2}}^{\mathrm{O_2}} = K_0\cdot\frac{\Delta P}{\Delta x} \quad (6)$$

Where $F_{\mathrm{O_2}}$ is total O_2 flux, $F_{\mathrm{O_2}}^{\mathrm{Mb}}$ is O_2 flux from Mb, $F_{\mathrm{O_2}}^{\mathrm{O_2}}$ is O_2 flux from free O_2, $P_{\mathrm{O_2}}$ is partial pressure of O_2 at the cell surface, P_{r} is $P_{\mathrm{O_2}}$ at the mitochondria (assumed to be 0), P_{50} is $P_{\mathrm{O_2}}$ that will half saturate Mb (O_2 binding affinity of Mb), C_{Mb} is Mb concentration, $\frac{\Delta P}{\Delta x}$ is $P_{\mathrm{O_2}}$ gradient from cell surface to the mitochondria, K_0 is Krogh's diffusion constant for free O_2, D_{Mb} is Mb diffusion coefficient.

The following equation describes the relative contribution to O_2 transport:

$$\frac{F_{\mathrm{O_2}}^{\mathrm{Mb}}}{F_{\mathrm{O_2}}^{\mathrm{O_2}}} = \frac{D_{\mathrm{Mb}}C_{\mathrm{Mb}}}{K_0(P_{\mathrm{O_2}}+P_{50})} \quad (7)$$

Statistical analysis

Statistical analysis, used Sigma Plot/Sigma Stat program (Systat Software, Inc.) and expressed the data as mean ± s.e.m. Linear least-squares regression determined the slopes, intercepts and correlation coefficients. Statistical significance was determined by two-tailed Student's t test ($P < 0.05$).

Results

Figure 1 shows the ^{1}H spectra of MbCO in solution measured with a modified PG-STE sequence at different gradient fields applied in the x direction. At 72.8 G, the Val E11 γ-methyl signal of MbCO at −2.4 ppm shows the lowest signal intensity (A in Fig. 1). As the gradient strength decreases from 63.7 to 18.2 G, the signal intensity rises. With applied field gradient 9.1 G, the signal intensity reaches its maximum intensity (H in Fig. 1). The analysis of the natural logarithm of the solution state MbCO and HbCO signal intensity as a function of the square of

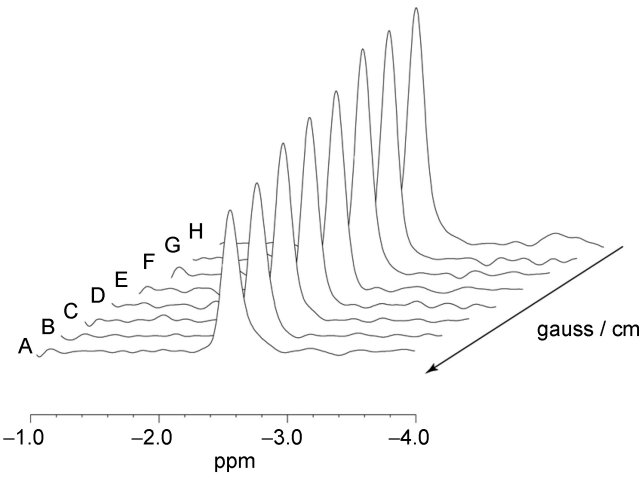

Figure 1. ^{1}H NMR diffusion-weighted spectra of MbCO solution at 22°C
A modified pulsed-field gradient stimulated echo (PG-STE) maps the gradient-dependent change in the γ CH_3 Val E11 MbCO signal at −2.4 ppm The signal intensity decreases as the applied field gradient increases. The bank of spectra shows changes with the incremental increase in field gradient strength applied stepwise in the x direction from (A–H) 72.8 to 9.1 G.

Table 1. Diffusion coefficients of Mb/Hb in solutions and in muscles

Sample	Method	$D \times 10^{-7}$ cm^2 s^{-1}	°C	Reference
MbCO solution (1.8 mM)	NMR	11.6*	22	This work
Mb diluted solution	Diffusion tube	11.3	20	(Riveros-Moreno & Wittenberg, 1972)
HbCO solution (0.75 mM)	NMR	7.53*	22	This work
HbCO solution (1.2 mM)	Diffusion tube	6.98	20	(Riveros-Moreno & Wittenberg, 1972)
Mb in rat myocardium	NMR, perfused heart	4.24*	22	This work
Mb in rat myocardium	NMR, calculated from rotation correlation time	5.0†	25	(Wang *et al.* 1997)
Model calculation	Literature data	23	37	(Federspiel, 1986)
18% Mb solution (~10 mM)	Diffusion across a thin porous plate	7.0	20	(Wittenberg, 1970)
Mb in undiluted homogenates of rat skeletal muscle	Multilayer diffusion	1.5	20	(Moll, 1968)
Mb injected into frog skeletal muscle	Fluorescence and photo-oxidation, microinjection of metMb	1.6	22	(Baylor & Pape, 1988)
Isolated rat soleus muscle fibre	Fluorescence and photo-oxidation, microinjection of metMb	1.25‡ 1.22§	22	(Jurgens *et al.* 1993; Papadopoulos *et al.* 2001)
Isolated rat cardiac muscle fibre	Fluorescence and photo-oxidation, microinjection of Fe^{+3} − Mb −H_2O (metMb)	1.17‡ 1.25§	22	(Jurgens *et al.* 1993; Papadopoulos *et al.* 2001)

Mb, myoglobin; Hb, haemaglobin; metMb. *Values calculated from best curve fit of data points in Figs 2 and 4. The radius of myoglobin is 17.5 Å (Kataoka *et al.* 1995). †The Stokes-Einstein equation connects the translational and rotational diffusion coefficients (Wang *et al.* 1997). ‡Axial direction of fibre. §Radial direction of fibre.

the gradient strength yields a translational diffusion coefficient of 11.6×10^{-7} cm^2 s^{-1} (1.8 mM Mb) and 7.53×10^{-7} cm^2 s^{-1} (0.75 mM Hb), calibrated against the H_2O diffusion coefficient 2.17×10^{-5} cm^2 s^{-1} (Fig. 2). The Mb and Hb diffusion coefficients match literature values (Table 1). Applying the field gradient along either the y or z direction yields identical diffusion coefficient values, as expected for an isotropic, homogeneous solution (data not shown).

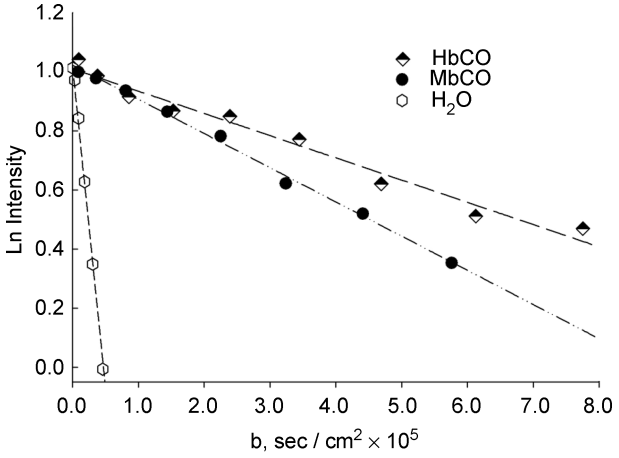

Figure 2. Plot of natural logarithm of the signal intensity of H_2O, γ CH3 Val E11 signal of MbCO and HbCO *versus* b ($\ln(\frac{S(G)}{S(0)}) = -bD = -\gamma^2 G^2 \delta^2 (\Delta - \delta/3) D$) with a field gradient applied in the x direction

Linear regression leads to the self-diffusion coefficient of 2.17×10^{-5} cm^2 s^{-1} (H_2O), 1.16×10^{-6} cm^2 s^{-1} (MbCO) and 7.53×10^{-7} cm^2 s^{-1} (HbCO) at 22°C, respectively. Field gradients applied in the y and z directions yield an identical set of diffusion coefficients. For definition of terms in equation, see text.

The perfused rat myocardium at 22°C shows physiological characteristics consistent with previously reported experiments (Table 2; Chung & Jue, 1999; Kreutzer & Jue, 2004). Introducing 30 mM KCl stops heart contraction. Rate pressure product (RPP) decreases from $10.9 \pm 0.4 \times 10^3$ mmHg min^{-1} to zero. During the period of K^+-induced arrest, oxygen consumption (MVO_2) decreases from 14.1 ± 0.6 to 5.0 ± 0.4 μmol min^{-1} (g dry weight)$^{-1}$ and ATP level decreases to 95.4 ± 1.6% of control. However, PCr rises to 120.6 ± 4.3% above the basal level. During reperfusion with control buffer, MVO_2 returns to 14.0 ± 1.0 μmol min^{-1} (g dry weight)$^{-1}$. PCr and ATP levels recover to 93.2 ± 3.2% and 93.9 ± 1.3% of the control level, respectively. RPP returns to $10.5 \pm 0.4 \times 10^3$ mmHg min^{-1}.

Figure 3 shows the ^{1}H spectra of the Val E11 γ-methyl signal of MbO_2 at −2.8 ppm from perfused myocardium measured with the same modified PG-STE sequence at different gradient fields applied in the y direction: 84.2 G (A) 74.8 G (B) 56.1 G (C) 37.4 G (D) and 4.7 G (E). At 84.2 G, the Val E11 γ-methyl signal of MbO_2 shows the lowest signal intensity. As the gradient strength decreases, the signal intensity increases.

A plot of the natural logarithm of the MbO_2 signal intensity from the myocardium ($n = 5$) as a function of the square of the gradient strength applied along x, y and z

Table 2. Physiological parameters for perfused heart at 22°C

	LVDP (mmHg)	HR (min^{-1})	RPP (mmHg min^{-1} $\times 10^3$)	MVO_2 (μmol min^{-1} (g dry wt)$^{-1}$)	PCr (%)	ATP (%)	*n*
Control	150.9 ± 7.2	72.3 ± 2.6	10.9 ± 0.4	14.1 ± 0.6	100	100	5
K^+-induced arrest	0	0	0	5.0 ± 0.4	120.6 ± 4.3	95.4 ± 1.6	5
Reperfusion	148.9 ± 8.4	71.0 ± 4.6	10.5 ± 0.7	14.0 ± 1.0	93.2 ± 3.2	93.9 ± 1.3	5

LVDP, left ventricular developed pressure; HR, heart rate; RPP, rate pressure product; MVO_2, oxygen consumption; PCr, phosphocreatine. Data are means ± S.E.M.

reveals a linear relationship (Fig. 4; $r > 0.99$). Gradients applied along *x*, *y* or *z* yield a similar translational diffusion coefficient: 4.12 ± 0.40 (*x*), 4.51 ± 0.38 (*y*) and 4.08 ± 0.19 (*z*) $\times 10^{-7}$ cm^2 s^{-1}. The average diffusion coefficient is therefore 4.24×10^{-7} cm^2 s^{-1}.

Figure 5 shows the relative contribution from Mb and free O_2 in transporting O_2 in the cell. The straight lines depict the contribution from free O_2 diffusion. The O_2 flux contribution from free O_2 diffusion reveals a linear dependence on P_{O_2} and has a slope that reflects the two values reported in the literature for the Krogh's diffusion constant (K_0) of 2.52 and 4.28×10^{-5} ml O_2 cm^{-1} min^{-1} atm^{-1}. The Mb-facilitated O_2 flux shows a concentration-dependent response based on the experimentally determined D_{Mb} value of 4.24×10^{-7} cm^2 s^{-1}. As Mb concentration increases from 0.19 to 0.42 mM, the Mb contribution to the overall O_2 flux increases correspondingly. Altering the P_{50} from 1.5 to 2.3 mmHg produces a modest change in the Mb-dependent O_2 flux. The intersection of the free O_2 and Mb-facilitated O_2 diffusion marks the equipoise diffusion P_{O_2}, where Mb and free O_2 contribute equally to the O_2 flux. Below the equipoise diffusion P_{O_2}, the Mb contribution dominates. Table 3 summarizes the equipoise diffusion P_{O_2} values at different Mb concentrations and values of P_{50} and K_0.

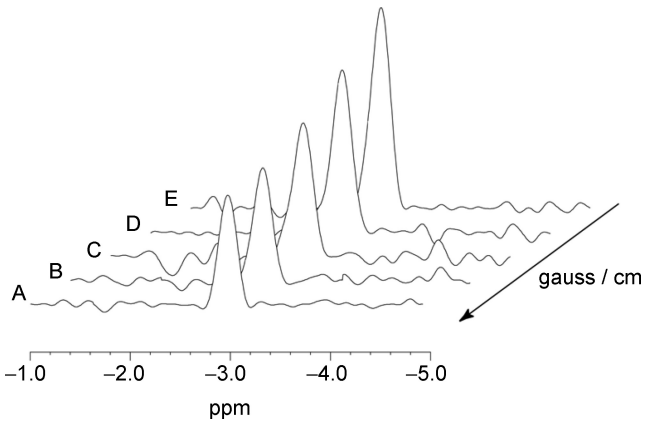

Figure 3. ^{1}H NMR diffusion-weighted spectra of MbO_2 from perfused rat heart under KCl-induced arrest at 22°C
A modified PG-STE sequence detects the peak intensity change in the MbO_2 γ CH3 Val E11 signal at −2.8 ppm as a function of gradient field strength in the *y* direction: 84.2 G, (A) 74.8 G, (B) 56.1 G, (C) 37.4 G, (D) and 4.7 G, (E).

Discussion

NMR signal of cellular MbO_2

With NMR, the detectable Val E11 MbO_2 signal in myocardium and skeletal muscle presents an opportunity to determine the endogenous Mb diffusion in the cell with pulsed-field gradient methodology. Control experiments confirm that the NMR-determined diffusion coefficients of solution Mb (11.6×10^{-7} cm^2 s^{-1}) and Hb (7.53×10^{-7} cm^2 s^{-1}) agree closely with values reported in the literature. In perfused myocardium, Mb diffusion in the cell drops by 37% from 11.6 to 4.24×10^{-7} cm^2 s^{-1}.

A comparative study has shown that the ^{1}H NMR spectral analysis and biochemical assay yield matching

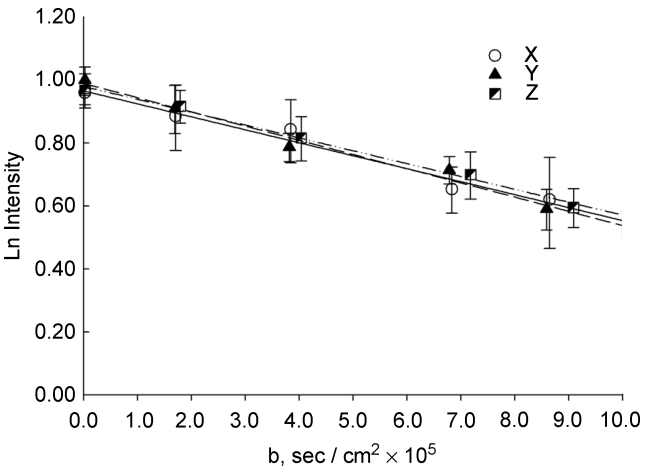

Figure 4. Plot of the natural logarithm of the MbO_2 Val E11 peak intensity from perfused heart as a function of *b*
Each point represents mean ± S.E.M. of the MbO_2 signal from perfused myocardium ($n = 5$). Standard error ranges from 3% to 14%. The MbO_2 signal an intensity decreases with each stepwise increase in gradient field strength in the *x*, *y* and *z* directions. In each of the three directions, the regression lines for the respective data points show no significant difference and lead to a translational diffusion coefficient of 4.12×10^{-7} cm^2 s^{-1} (A) in the *x* direction, 4.51×10^{-7} cm^2 s^{-1} (B) in the *y* direction and 4.08×10^{-7} cm^2 s^{-1} (C) in the *z* direction.

Table 3. Equipoise diffusion P_{O_2} in tissue with different Mb concentration

	$K_0 = 2.52 \times 10^{-5}$ ml O_2 cm^{-1} min^{-1} atm^{-1} (at 23°C)		$K_0 = 4.28 \times 10^{-5}$ ml O_2 cm^{-1} min^{-1} atm^{-1} (at 23°C)	
	P_{50} (1.5 mmHg) (mmHg)	P_{50} (2.3 mmHg) (mmHg)	P_{50} (1.5 mmHg) (mmHg)	P_{50} (2.3 mmHg) (mmHg)
P_{O_2} (0.19 mM Mb)	1.77	0.97	0.42	—
P_{O_2} (0.42 mM Mb)	5.72	4.92	2.76	1.96
P_{O_2} (1.4–4.0 mM Mb)	22.58–67.30	21.78–66.50	12.69–39.03	11.89–38.23

Equipoise diffusion P_{O_2} is defined as the P_{O_2} that allows Mb and O_2 to contribute equally to O_2 transport. P_{50} is the P_{O_2} that half saturates Mb.

values for the Mb concentration in the perfused rat myocardium. No significant bound pool of Mb exists in the cell, and the NMR Mb Val E11 signal reflects the total cellular Mb pool (Kreutzer *et al.* 1993). Moreover, the line shape of the Mb Val E11 signal in the cell *versus* in solution shows no significant deviation, consistent with freely diffusing Mb pool in the cell. Any significant compartmentalization or restricted diffusion of Mb would yield disparate NMR *versus* biochemical assay results and contrasting solution *versus* cellular Mb line shapes.

Under normoxic conditions, the perfused myocardium model in the study also reveals no sign of O_2 heterogeneity, which would give rise to a regional distribution of partially saturated MbO_2 (Kreutzer & Jue, 1995). Experiments with infused high affinity CO yield a dynamically matching MbCO and MbO_2 Val E11 signal intensity. The MbCO signal intensity never exceeds the MbO_2 signal intensity, and the sum of the MbCO and MbO_2 signal remains constant (Glabe *et al.* 1998; Chung *et al.* 2006). Any O_2 heterogeneity would yield a higher MbCO signal intensity.

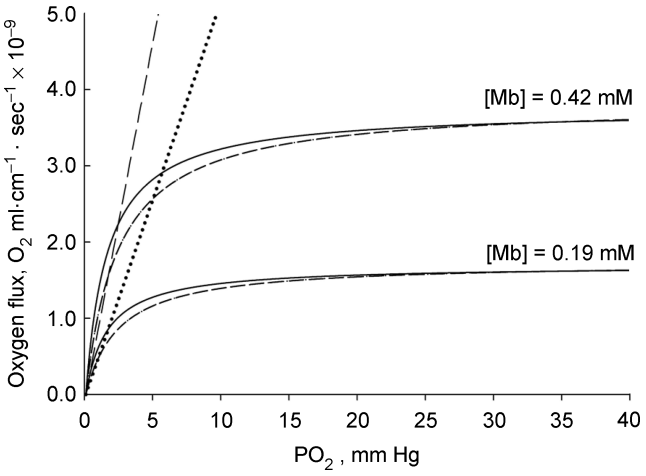

Figure 5. Plot of free O_2 flux *versus* Mb-facilitated O_2 diffusion as a function of P_{O_2} at 22°C
The free O_2 flux increases linearly with P_{O_2}. Two lines show the rate of change given as cellular free O_2 diffusion constant of $K_0 = 4.28 \times 10^{-5}$ (dashed line) and $K_0 = 2.52 \times 10^{-5}$ (dotted line) ml O_2 cm^{-1} min^{-1} atm^{-1}. The two non-linear curves show the O_2 flux contribution from Mb-facilitated diffusion increases as the cellular Mb concentration rises from 0.19 to 0.42 mM. The contribution of Mb-facilitated O_2 diffusion also increases when the P_{50} decreases from 2.3 (dashed line) to 1.5 mmHg (continuous line).

Comparison of translational diffusion coefficients

The literature contains reports of D_{Mb} ranging from 1.2 to 23×10^{-7} cm^2 s^{-1} (Riveros-Moreno & Wittenberg, 1972; Federspiel, 1986; Papadopoulos *et al.* 1995). Many models have predicted on the premise that the Mb concentration in terrestrial mammalian muscle does not exceed 0.5 mM and the cellular environment contains enzymes as well as metabolites that increase the viscosity. As a consequence, the D_{Mb} of an 18 g dl^{-1} Mb solution (5–7 $\times 10^{-7}$ cm^2 s^{-1} at 20°C) has served as a key starting point for mathematical modelling of intracellular O_2 transport (Riveros-Moreno & Wittenberg, 1972; Federspiel, 1986). To mimic the cellular environment, tissue homogenates have been used. In rat skeletal muscle homogenate, Fe (+3) Mb-H_2O (metMb) has a D_{Mb} of 1.5×10^{-7} cm^2 s^{-1} at 20°C (Moll, 1968). Homogenates, however, do not necessarily reflect the cellular milieu. Indeed, the literature has documented, such as the case with ADP, that homogenates and the cell do not exhibit matching free metabolite and enzyme pools (Iles *et al.* 1985).

Nevertheless, studies following the diffusion of microinjected metMb into Mb-free frog muscle have found a similar D_{Mb} of 1.6×10^{-7} cm^2 s^{-1} at 22°C (Baylor & Pape, 1988). Similarly, recent fluorescence recovery after photobleaching (FRAP) experiments have followed the diffusion of microinjected dye-conjugated metMb in isolated muscle fibre from heart and skeletal muscle tissue and have obtained a D_{Mb} of 1.2×10^{-7} cm^2 s^{-1} at 22°C, which is about 10 times slower than dilute Mb diffusion (Papadopoulos *et al.* 2001). Because of the uncertain contribution of metMb reaction kinetics with Mb reductase, the non-physiological nature of an isolated fibre model, and boundary condition assumptions, questions have been raised about the validity of the observed D_{Mb} as a reflection of endogenous Mb diffusion in respiring tissue (Groebe, 1995). In particular, invasive microinjection procedure requires 4–6 h of post-injection recovery to minimize cell trauma (Seksek *et al.* 1997). The present NMR study shows that the endogenous Mb

diffusion in respiring myocardium has a D_{Mb} 2.7 times slower than dilute Mb solution, but about 2.7–3.5 times faster than the diffusion coefficient determined by Mb microinjection-based experiments.

Mb *versus* free O_2 contribution to O_2 flux

A key element of the Mb-facilitated diffusion theory pivots about the translational diffusion of Mb in the cell. The intracellular O_2 transport depends upon the O_2 flux from Mb and free O_2, FO_2^{Mb} and $FO_2^{O_2}$, (eqns (4–7)). A relatively low diffusion coefficient of Mb in the cell cannot support a significant role for Mb in facilitating O_2 diffusion, as Mb cannot compete effectively with free O_2 diffusion.

The contribution from free O_2 flux depends linearly upon P_{O_2} and K_0. K_0 values ranging from 2.52 to 4.28×10^{-5} ml O_2 cm^{-1} min^{-1} atm^{-1} have been reported (Bentley *et al.* 1993). With a K_0 of 2.52×10^{-5} ml O_2 cm^{-1} min^{-1} atm^{-1}, a P_{50} of 1.5 mmHg and an Mb concentration of 0.19 mM, the NMR-determined translational diffusion coefficient of 4.24×10^{-7} cm^2 s^{-1} yields an equipoise diffusion P_{O_2} of 1.77 mmHg, where Mb and free O_2 have equal contribution to the O_2 flux. Below a P_{O_2} of 1.77 mmHg, the Mb-dependent contribution to the O_2 flux begins to dominate. Increasing the concentration of Mb from 0.19 to 0.42 mM shifts the equipoise diffusion P_{O_2} to 5.7 mmHg, well above the Mb P_{50}. In essence, as Mb concentration rises, its role in facilitated O_2 diffusion also increases.

In terrestrial mammalian muscle, the Mb concentration range from 0.19 mM in heart muscle to 0.42 mM in soleus muscle indicates a higher poise for Mb-facilitated O_2 diffusion in skeletal muscle than in myocardium (Wittenberg, 1970). In marine mammalian muscle, Mb concentration in muscle can rise to 25–70 g (kg tissue)$^{-1}$ (approximately 1.4–4 mM) (Dolar *et al.* 1999; Wright & Davis, 2006). At 1.4–4 mM Mb, the equipoise diffusion P_{O_2} increases to 12–38 mmHg at 37°C. Mb-dependent O_2 diffusion predominates even under resting conditions.

In vivo NMR experiments have shown that in the basal state of muscle, sufficient O_2 exists to saturate Mb $> 90\%$ and to keep the P_{O_2} well above 10 mmHg. Even as myocardial respiration increases with workload, the O_2 level does not fall enough to produce a detectable deoxy-Mb signal (Zhang *et al.* 1999; Kreutzer *et al.* 2001). No transient fluctuation in MbO_2 saturation appears in a cardiac contraction cycle (Chung & Jue, 1999). Moreover, spontaneously beating heart with 77% of Mb inactivated with CO suffers no impairment in respiration, contractile function or high energy phosphate state, even under conditions that would accentuate the purported role of Mb in O_2-facilitated diffusion (Glabe *et al.* 1998; Chung *et al.* 2006). Mb does not appear to play a significant role in regulating myocardial respiration.

In contrast, as skeletal muscle begins to contract, Mb desaturates within 30 s to reach a deoxygenated steady state that depends upon workload, even though the cell has abundant O_2 to drive oxidative phosphorylation (Mole *et al.* 1999; Chung *et al.* 2005). MbO_2 responds to a transient rather than a steady-state change in energy demand.

As the Mb P_{50} rises, however, the equipoise diffusion P_{O_2} declines. In particular, during muscle contraction, the muscle temperature rises and will increase the Mb P_{50} (Schenkman *et al.* 1997). If Mb P_{50} rises from 1.5 to 2.3 mmHg, the equipoise diffusion P_{O_2} decreases from 1.77 to 0.97 mmHg in tissue with 0.19 mM Mb. At 0.42 mM Mb, the equipoise diffusion P_{O_2} shifts from 5.72 to 4.92 mmHg. As muscle contraction proceeds and generates heat, the cell reduces its reliance on Mb-facilitated O_2 diffusion.

Isotropic *versus* anisotropic diffusion

In solution, Mb exhibits isotropic diffusion; in myocyte, Mb can exhibit anisotropic diffusion, as the longitudinal myofibril dimension exceeds the radial dimension by a factor of 10. In particular, the different fibre orientations in the myocardium could lead to a macroscopic volume-averaged determination of the components of the apparent diffusion tensor. Indeed, de Graaf *et al.* (2000) have hinted at anisotropic diffusion of PCr and ATP in the sarcoplasm. For Mb, however, the translational diffusion in the cell shows no orientation preference. In the x, y and z directions, Mb diffuses at 4.12 ± 0.40, 4.51 ± 0.38 and $4.08 \pm 0.19 \times 10^{-7}$ cm^2 s^{-1}, respectively.

The isotropic motion of Mb agrees with the independent rotational diffusion analysis. Because paramagnetic molecules can exhibit field-dependent relaxation, the deoxy-Mb proximal histidyl $N_\delta H$ signal has served to assess Mb rotational diffusion time in respiring muscle tissue. Under the assumption of unrestricted, isotropic diffusion, the observed rotational correlation time of $13.6 \pm 1.3 \times 10^{-9}$ s leads to a calculated translational diffusion coefficient of $4–6 \times 10^{-7}$ cm^2 s^{-1} (Wang *et al.* 1997). The calculated and measured translational diffusion values are in excellent agreement. Mb diffusion does not distinguish between the radial *versus* axial direction and shows an apparent isotropic motion.

Estimated root mean square (RMS) displacement

Previous studies have used the O_2 off-rate constant for MbO_2 and the translational diffusion coefficient to estimate the RMS displacement (Wittenberg & Wittenberg, 2003). For Mb, the rate determining O_2 off-rate has served as a basis to estimate the O_2 residence time. Beyond the RMS displacement, Mb will lose half of its O_2 load. At 20°C, the MbO_2 dissociation constant

of $12\,s^{-1}$ leads to a half-time ($t_{1/2}$) of approximately 58 ms, the time required to dissociate half of the O_2 from MbO_2 (Gibson *et al.* 1986). Given the measured D_{Mb} of $4.24 \times 10^{-7}\,cm^2\,s^{-1}$, the Einstein-Smoluchowski equation of the mean square displacement, $\langle r^2 \rangle = 6Dt$, yields a RMS displacement of $\langle r \rangle = 3.8\,\mu m$ (Wittenberg & Wittenberg, 2003). As muscle cells have a typical dimension of $10\,\mu m \times 100\,\mu m$, a RMS displacement of Mb represents a small portion of the cell. Electron microscopy analysis reveals that many mitochondria cluster near the capillary and form a reticulum. A $3.8\,\mu m$ Mb RMS displacement poses no apparent limitation of O_2 delivery to the mitochondria reticulum (Kirkwood *et al.* 1986).

Cellular architecture

The Mb diffusion coefficients also yield insight into the cellular environment and architecture. Field-dependent relaxation measurement of the paramagnetic proximal histidyl $N_\delta H$ Mb signal reveals an Mb rotational correlation time about 1.4 times longer in the myocardium cell than in solution and an estimate of the translational diffusion coefficient ($4–6 \times 10^{-7}\,cm^2\,s^{-1}$) (Wang *et al.* 1997). Independent pulsed-field gradient method confirms that indeed Mb diffuses in the myocardial cell at $4.24 \times 10^{-7}\,cm^2\,s^{-1}$. Both measurements point to a local cellular environment that slows Mb diffusion by about 40% relative to solution Mb (1.8 mM). Calibrating the diffusion against the water or Mb solution viscosity of 0.95 cP (centipoise) at 22°C leads to a cardiac myocyte viscosity of 2.6 cP, 2.74 times larger than solution viscosity (Lide & Frederikse, 1990). Indeed, the NMR and FRAP portrayal of the cellular architecture shares similar features. FRAP experiments have determined a cellular viscosity in the 2–3 cP range, in excellent agreement with the values derived from NMR rotational and translational diffusion measurements (Mastro *et al.* 1984). The translational diffusion of large solutes in cytoplasm and nucleus slows only 3–4 times relative to water diffusion and indicates an unrestricted diffusion distance of $\sim 4\,\mu m$ in the cell (Kao *et al.* 1993). The NMR-determined Mb diffusion provides then another perspective and experimental means to assess any impact of cellular crowding on enzyme reactivity (Welch & Marmillot, 1991).

Conclusion

This study has applied pulsed-field gradient NMR methods to determine the endogenous Mb diffusion in perfused rat myocardium. Mb diffuses with a translational diffusion coefficient of $4.24 \times 10^{-7}\,cm^2\,s^{-1}$ and shows no orientation preference over an estimated RMS displacement of $3.8\,\mu m$. The translational diffusion coefficient matches precisely the value predicted by previous rotational diffusion measurements. Comparing the flux contribution from free O_2 *versus* Mb reveals an equipoise diffusion P_{O_2} of 1.77 mmHg in rat myocardium and 5.72 mmHg in rat skeletal muscle. In marine mammalian muscle, the equipoise diffusion P_{O_2} can increase to 67 mmHg. The different equipoise diffusion P_{O_2} values arise largely from a variation in Mb concentration. Altering the P_{50} induces only a modest change. For terrestrial mammals, Mb can contribute to the O_2 flux only if intracellular P_{O_2} falls significantly, especially with increased energy demand.

References

Baylor SM & Pape PC (1988). Measurement of myoglobin diffusivity in the myoplasm of frog skeletal muscle fibres. *J Physiol* **406**, 247–275.

Bentley TB, Meng H & Pittman RN (1993). Temperature-dependence of oxygen diffusion and consumption in mammalian striated-muscle. *Am J Physiol Heart Circ Physiol* **264**, H1825–H1830.

Chung Y, Glabe A & Huang SJ (2006). Impact of myoglobin inactivation on myocardial function. *Am J Physiol Cell Physiol* **290**, C1616–C1624.

Chung Y & Jue T (1996). Cellular response to reperfused oxygen in the postischemic myocardium. *Am J Physiol Heart Circ Physiol* **271**, H687–H695.

Chung Y & Jue T (1999). Regulation of respiration in myocardium in the transient and steady state. *Am J Physiol Heart Circ Physiol* **277**, H1410–H1417.

Chung Y, Mole PA, Sailasuta N, Tran TK, Hurd R & Jue T (2005). Control of respiration and bioenergetics during muscle contraction. *Am J Physiol Cell Physiol* **288**, C730–C738.

de Graaf RA, van Kranenburg A & Nicolay K (2000). In vivo P-31-NMR diffusion spectroscopy of ATP and phosphocreatine in rat skeletal muscle. *Biophys J* **78**, 1657–1664.

Dolar ML, Suarez P, Ponganis PJ & Kooyman GL (1999). Myoglobin in pelagic small cetaceans. *J Exp Biol* **202**, 227–236.

Federspiel WJ (1986). A model study of intracellular oxygen gradients in a myoglobin-containing skeletal muscle fiber. *Biophys J* **49**, 857–868.

Garry DJ, Ordway GA, Lorenz JN, Radford NB, Chin ER, Grange RW, Bassel-Duby R & Williams RS (1998). Mice without myoglobin. *Nature* **395**, 905–908.

Gibson QH, Olson JS, McKinnie RS & Rohlfs RJ (1986). A kinetic description of ligand binding to sperm whale myoglobin. *J Biol Chem* **261**, 10228–10239.

Gimenez M, Sanderson RJ, Reiss OK & Banchero N (1977). Effects of altitude on myoglobin and mitochondrial protein in canine skeletal muscle. *Respiration* **34**, 171–176.

Glabe A, Chung Y, Xu D & Jue T (1998). Carbon monoxide inhibition of regulatory pathways in myocardium. *Am J Physiol Heart Circ Physiol* **274**, H2143–H2151.

Godecke A, Flogel U, Zanger K, Ding Z, Hirchenhain J, Decking UK & Schrader J (1999). Disruption of myoglobin in mice induces multiple compensatory mechanisms. *Proc Natl Acad Sci U S A* **96**, 10495–10500.

Groebe K (1995). An easy-to-use model for O_2 supply to red muscle. Validity of assumptions, sensitivity to errors in data. *Biophys J* **68**, 1246–1269.

Guyton GP, Stanek KS, Schneider RC, Hochachka PW, Hurford WE, Zapol DG, Liggins GC & Zapol WM (1995). Myoglobin saturation in free-diving Weddell seals. *J Appl Physiol* **79**, 1148–1155.

Haase A, Frahm J, Hanicke W & Matthaei D (1985). H-1-NMR chemical-shift selective (CHESS) imaging. *Phys Med Biol* **30**, 341–344.

Iles RA, Stevens AN, Griffiths JR & Morris PG (1985). Phosphorylation status of the liver by ^{31}P NMR spectroscopy and its implications for metabolic control. *Biochem J* **229**, 141–151.

Johnson RL, Heigenhauser GJF, Hsia CCW, Jones NL & Wagner PD (1996). Determinants of gas exchange and acid-base balance during exercise. In *Exercise, Regulation and Integration of Multiple Systems*, ed. Rowell LB & Shepher JT, pp. 515–584. Oxford University Press, New York.

Jurgens KD, Peters T & Gros G (1993). Diffusivity of myoglobin in intact skeletal muscle cells. *Proc Natl Acad Sci U S A* **91**, 3829–3833.

Kao HP, Abney JR & Verkman AS (1993). Determinants of the translational mobility of a small solute in cell cytoplasm. *J Cell Biol* **120**, 175–184.

Kataoka M, Nishii I, Fujisawa T, Ueki T, Tokunaga F & Goto Y (1995). Structural characterization of the molten globule and native states of apomyoglobin by solution X-ray-scattering. *J Mol Biol* **249**, 215–228.

Kirkwood SP, Munn EA & Brooks GA (1986). Mitochondrial reticulum in limb skeletal muscle. *Am J Physiol Cell Physiol* **251**, C395–C402.

Kooyman GL & Ponganis PJ (1998). The physiological basis of diving to depth: birds and mammals. *Annu Rev Physiol* **60**, 19–32.

Kreutzer U, Chung Y, Butler D & Jue T (1993). ^{1}H-NMR characterization of the human myocardium myoglobin and erythrocyte hemoglobin signals. *Biochim Biophys Acta* **1161**, 33–37.

Kreutzer U & Jue T (1995). Critical intracellular oxygen in the myocardium as determined with the 1H NMR signal of myoglobin. *Am J Physiol Heart Circ Physiol* **268**, H1675–H1681.

Kreutzer U & Jue T (2004). The role of myoglobin as a scavenger of cellular NO in myocardium. *Am J Physiol Heart Circ Physiol* **286**, H985–H991.

Kreutzer U, Mekhamer Y, Chung Y & Jue T (2001). Oxygen supply and oxidative phosphorylation limitation in rat myocardium in situ. *Am J Physiol Heart Circ Physiol* **280**, H2030–H2037.

Kreutzer U, Wang DS & Jue T (1992). Observing the ^{1}H NMR signal of the myoglobin Val-E11 in myocardium: an index of cellular oxygenation. *Proc Natl Acad Sci U S A* **89**, 4731–4733.

Lide DR & Frederikse HPR (1990). *CRC Handbook of Chemistry and Physics*, 71st edn. pp. 2512 CRC Press, Boca-Raton.

Livingston DJ, La Mar GN & Brown WD (1983). Myoglobin diffusion in bovine heart muscle. *Science* **220**, 71–73.

Mastro AM, Babich MA, Taylor WD & Keith AD (1984). Diffusion of a small molecule in the cytoplasm of mammalian cells. *Proc Natl Acad Sci U S A* **81**, 3414–3418.

Mole PA, Chung Y, Tran TK, Sailasuta N, Hurd R & Jue T (1999). Myoglobin desaturation with exercise intensity in human gastrocnemius muscle. *Am J Physiol Regul Integr Comp Physiol* **277**, R173–R180.

Moll W (1968). The diffusion coefficient of myoglobin in muscle homogenate. *Pflugers Arch Gesamte Physiol Menschen Tiere* **299**, 247–251.

Papadopoulos S, Endeward V, Revesz-Walker B, Jurgens KD & Gros G (2001). Radial and longitudinal diffusion of myoglobin in single living heart and skeletal muscle cells. *Proc Natl Acad Sci U S A* **98**, 5904–5909.

Papadopoulos S, Jurgens KD & Gros G (1995). Diffusion of myoglobin in skeletal muscle cells - dependence on fibre type, contraction and temperature. *Pflugers Arch* **430**, 519–525.

Ponganis PJ, Kreutzer U, Sailasuta N, Knower T, Hurd R & Jue T (2002). Detection of myoglobin desaturation in Mirounga angustirostris during apnea. *Am J Physiol Regul Integr Comp Physiol* **282**, R267–R272.

Price WS (1997). Pulsed-field gradient nuclear magnetic resonance as a tool for studying translational diffusion.1. Basic theory. *Concepts Magnetic Resonance* **9**, 299–336.

Riveros-Moreno V & Wittenberg JB (1972). The self-diffusion coefficients of myoglobin and hemoglobin in concentrated solution. *J Biol Chem* **247**, 895–901.

Schenkman KA, Marble DR, Burns DH & Feigl EO (1997). Myoglobin oxygen dissociation by multiwavelength spectroscopy. *J Appl Physiol* **82**, 86–92.

Seksek O, Biwersi J & Verkman AS (1997). Translational diffusion of macromolecule-sized solutes in cytoplasm and nucleus. *J Cell Biol* **138**, 131–142.

Stejskal EO & Tanner JE (1965). Spin diffusion measurements: spin echoes in the presence of a time-dependent field gradient. *J Chem Phys* **42**, 288–292.

Terrados N, Jansson E, Sylven C & Kaijser L (1990). Is hypoxia a stimulus for synthesis of oxidaative enzymes and myoglobin? *J Appl Physiol* **68**, 2369–2372.

Wang D, Kreutzer U, Chung Y & Jue T (1997). Myoglobin and hemoglobin rotational diffusion in the cell. *Biophys J* **73**, 2764–2770.

Welch GR & Marmillot PR (1991). Metabolic 'channeling' and cellular physiology. *J Theor Biol* **152**, 29–33.

Wittenberg BA & Wittenberg JB (1989). Transport of oxygen in muscle. *Annu Rev Physiol* **51**, 857–878.

Wittenberg JB (1970). Myoglobin-facilitated oxygen diffusion: role of myoglobin in oxygen entry into muscle. *Physiol Rev* **50**, 559–636.

Wittenberg JB & Wittenberg BA (2003). Myoglobin function reassessed. *J Exp Biol* **206**, 2011–2020.

Wright TJ & Davis RW (2006). The effect of myoglobin concentration on aerobic dive limit in a Weddell seal. *J Exp Biol* **209**, 2576–2585.

Zhang J, Murakami Y, Zhang Y, Cho Y, Ye Y, Gong G, Bache R, Ugurbil K & From AH (1999). Oxygen delivery does not limit cardiac performance during high work states. *Am J Physiol Heart Circ Physiol* **276**, H50–H57.

Acknowledgements

We gratefully acknowledge funding support from NIH GM 58688 (T.J.), Philip Morris 005510 (T.J.) and American Heart Association Western States Affiliate 0265319Y (U.K.) and the invaluable technical assistance of Drs Jeff Walton and Jeff de Ropp.